Oscillator-AC: Restoring Rigour to Linearized Small-Signal Analysis of Oscillators

Ting Mei and Jaijeet Roychowdhury
{meiting,jr}@ece.umn.edu
University of Minnesota, Twin Cities, USA

***Abstract*— Standard small-signal analysis methods for circuits break down for oscillators because small input perturbations result in arbitrarily large output changes, thus invalidating fundamental assumptions for small-signal analysis. In this paper, we propose a novel oscillator-AC (OAC) approach remedying this situation, thus restoring validity and rigour to small-signal analysis of oscillators. Our approach centers around a novel, general equation formulation for circuits that we term the GeMPDE. A key feature of our approach is to solve for *bivariate frequency variables* with the help of novel augmenting *phase condition* equations. Our GeMPDE-based small-signal analysis provides both amplitude and frequency characteristics in a unified manner and is applicable to any kind of oscillator described by differential equations. We obtain speedups of 1–2 orders of magnitude over the transient simulation approach commonly used today by designers for oscillator perturbation analysis. We also demonstrate and explain how our linearization approach captures the inherently *nonlinear* phenomenon of injection locking in oscillators.**

I. Introduction

Oscillators are building blocks in electronic, mechanical, optical and many other types of engineering systems. Examples of oscillators include voltage-controlled oscillators (VCOs), digital clocks, phase-locked loops, motors, engines, lasers, *etc.*. Analysis of the effects of small perturbations on oscillators is an important practical and theoretical problem. Small perturbations can, for example, lead to thickening of the oscillator's frequency spectrum (an effect known as *phase noise*), or to uncertainties in the locations of switching edges (known as *timing jitter*) in clocked systems. Effects of such non-idealities include degradation of throughput and bit-error rate (BER) in communication systems, and the need for lower clock speeds in computer systems.

In recent years, the sources of perturbations to oscillator-based systems have grown in variety. In addition to intrinsic device noise perturbations, interference "noise" from imperfect power supply/ground lines and chip substrates have become of substantial concern to designers. Correct and speedy analysis of oscillators under small perturbations has therefore become of great importance in practice. Frequency sweeps akin to standard small-signal analysis are of particular value to designers interested in obtaining metrics of oscillator sensitivity to interference frequency.

Unfortunately, standard small-signal analysis, such as that used for AC and noise analysis in SPICE [1], [2], is not applicable to oscillators. The reason is that oscillators are different from most other electronic circuits, in that *small* perturbations to them lead to *large* changes in phase and timing properties [3]. As a result, the underlying assumption of linearization in small-signal analysis, that output changes always remain small, breaks down for oscillators. The numerical manifestation of this fundamental property of oscillators is ill-conditioning and singularity of small-signal analysis matrices.

In the absence of the "usual" small-signal analysis capability of SPICE, designers are currently forced to resort to full transient analysis for oscillator simulations. However, as is well known, transient analysis has peculiar disadvantages for oscillators. The tradeoff between accuracy of results and step-size is much worse for oscillators than for non-oscillatory circuits like amplifiers and mixers. In particular, small numerical errors in phase accumulate without limit, resulting in unacceptable accuracy, unless extremely small timesteps ($\sim$400-1000 timesteps per cycle, typically, for a simulation length of $\sim$100 cycles) are taken. This makes transient simulation very much slower than a potential AC analysis, especially when a frequency sweeps are desired: for transient, an entire nonlinear simulation is required for each frequency (followed by postprocessing), while the single complex-matrix solution of AC analysis provides the same information more accurately. Therefore, it is very desirable to restore validity and rigour to small-signal analysis for oscillators.

AC analysis [1], [2] (*i.e.*, linearized small-signal frequency domain analysis) has long been used to efficiently analyze sinusoidal (or periodic) steady-state responses of linear time invariant (LTI) circuits. AC analyses are a staple for analog designers, who apply it to circuits such as amplifiers, first linearizing the nonlinear circuits about a DC operating point. The concept of AC analysis has also been profitably extended to nonlinear circuits operating in large-signal periodic steady-state, such as mixers and switched-capacitor filters (*e.g.*, [4]–[7]). This linear periodic time-varying (LPTV) AC analysis can capture important aspects of periodically-driven circuits, such as frequency translation and sampling. Neither LTI nor LPTV AC analysis is applicable to oscillators; if applied blindly, breakdown due to ill-conditioning or outright singularity of the AC matrices results.

Recently, a class of techniques based on the concept of multi-time partial differential equations (MPDEs) have been proposed and used to efficiently simulate systems with widely separated time scales, *i.e.*, with fast/slow characteristics. In the MPDE formulation, signal components with different rates of variation are represented by their "own" artificial time variables [8], [9]. An extension (the Warped MPDE or WaMPDE) of MPDE methods has also been proposed [10] that is able to better analyze amplitude and frequency modulation in oscillators. In the WaMPDE, some time scales are dynamically rescaled (warped time) to make the undulation of FM signal uniform. The concept of time warping introduced in the WaMPDE has been further generalized [10] to obtain a family of equation formulations collectively termed the Generalized MPDE, or GeMPDE. A key characteristic of the GeMPDE is that it features "local frequency" variables which are themselves functions of multiple time scales. These local frequencies are linked to multi-time "phase variables" through nonlinear, implicit ODEs.

In this paper, we propose a novel and unified approach for small signal or "AC" analysis of oscillators by exploiting a special case of the GeMPDE. In this particular GeMPDE formulation, the frequency is treated as an extra explicit variable with two time scales — an internal "warped" scale and an external "unwarped" time scale. A set of extra equations, which we term *phase conditions*, are proposed and added to the system to make the numbers of equations and unknowns the same, thus making it possible to obtain a unique solution. One of the effects of using this bi-variate frequency variable is to separate changes in amplitude and frequency, both of which always remain small if the external perturbation is small. Therefore, linear small signal analysis of this special GeMPDE becomes valid. The numerical manifestation of this fact is a well-posed Jacobian matrix that remains comfortably nonsingular at all frequencies, as we prove.

By restoring validity to small signal analysis of oscillators with the GeMPDE formulation, our method achieves large speedups over transient solution, just as traditional AC analysis does for non-oscillatory systems. While our linearized oscillator analysis relies on multi-time computations for all the "hard work", "normal" time-domain waveforms are easily recovered through simple and fast postprocessing. The postprocessing step involves solution of a *scalar* nonlinear ODE that relates multi-time frequency and single-time phase variables. Our method provides both frequency and amplitude variations in a unified manner from the small-signal transfer function

0-7803-9254-X/05/$20.00 ©2005 IEEE.

calculated, and is applicable to any kind of oscillator.

We demonstrate our OAC method on a variety of LC and ring oscillators in this paper. OAC analysis results show perfect agreement with SPICE-like full transient simulation, as expected, but provide speedups of 1-2 orders of magnitude. Furthermore, results show that OAC can predict injection locking [11], [12] accurately. OAC captures this nonlinear phenomenon via the scalar postprocessing nonlinear ODE solution that bridges multi-time and single-time solutions.

The remainder of the paper is organized as follows. In Section II, we review the rank-deficiency problem in the frequency-domain conversion matrix of oscillators for the DAE/MPDE and WaMPDE formulations. In Section III, we propose a well-posed GeMPDE formulation and novel augmenting phase conditions. We also prove the nonsingularity of GeMPDE's linearization and present the OAC technique in this section. In Section IV, we apply OAC to a number oscillator circuits of different kinds, demonstrating improvements in computation time over transient, as well as its ability to predict injection locking.

II. Rank-deficiency in previous oscillator linearization approaches

Standard small-signal analysis is not applicable to oscillators because of their fundamental property of neutral phase stability, resulting in singularity of small-signal matrices. In this section, we first demonstrate the rank-deficiency problem in the DAE/MPDE frequency-domain conversion matrix of oscillators. We then demonstrate how the WaMPDE formulation [10] succeeds in correcting the problem at DC but fails to do so at all other harmonics[1].

A. Preliminaries

Oscillator circuits under perturbation can be described by the DAE system

$$\frac{dq(x)}{dt} + f(x) = Au(t), \tag{1}$$

where $u(t)$ is a small perturbation signal, $x(t)$ is a vector of circuit unknowns (node voltages and branch currents), and A is an incidence matrix that captures the connection of the perturbation to the circuit. It has been shown in [3] that small perturbations applied to orbitally-stable oscillators can lead to dramatic changes in output, thus invalidating the fundamental assumption of small-signal analysis, *i.e.*, that output changes always remain small.

To more conveniently perform small-signal analysis of the oscillator, we first recall the MPDE [8], [9] forms of (1), which separate the input and system time scales. This leads to a form of the linear time varying (LTV) transfer function useful for small-signal analysis, as we show shortly. The MPDE form of (1) is

$$\left[\frac{\partial}{\partial t_1} + \frac{\partial}{\partial t_2}\right] q(\hat{x}(t_1,t_2)) + f(\hat{x}(t_1,t_2)) = Au(t_1). \tag{2}$$

$\hat{x}(t_1,t_2)$ is the bivariate form of $x(t)$ in (1).

We will also need the Warped MPDE (WaMPDE) formulation [10], an extension of the MPDE that originally proposed to address efficiency problems the MPDE faces when encountering strong frequency modulation (FM) in oscillators. Following [10], the WaMPDE corresponding to (1) is

$$\left[\frac{\partial}{\partial t_1} + \omega(t_1)\frac{\partial}{\partial t_2}\right] q(\hat{x}) + f(\hat{x}) = Au(t_1), \tag{3}$$

where $\omega(t_1)$ is a changing local frequency variable. t_2 is a dynamically rescaled (warped) time scale which makes the undulation of frequency modulation uniform. Using the WaMPDE form separates changes in amplitude and frequency and, as will become clear later, helps alleviate the rank-deficiency problem in the frequency-domain small-signal analysis matrix of oscillators to some extent.

[1]Due to space limitations, we are compelled to omit proofs.

B. Singularity of MPDE conversion matrix at frequencies $s = ij\omega_0, \forall i$

We assume that $x^*(t_2)$ is the unperturbed steady-state oscillatory solution of (2), *i.e.*, the solution when $u(t_1) = 0$. Linearizing the MPDE (2) around $x^*(t_2)$, we obtain

$$\left[\frac{\partial}{\partial t_1} + \frac{\partial}{\partial t_2}\right] (C(t_2)\Delta\hat{x}) + G(t_2)\Delta\hat{x} = Au(t_1). \tag{4}$$

Here, $C(t_2) = (\partial q(\hat{x})/\partial\hat{x})|_{x^*}$ and $G(t_2) = (\partial f(\hat{x})/\partial\hat{x})|_{x^*}$. Performing a Laplace transform with respect to t_1, we further obtain

$$\left[s + \frac{\partial}{\partial t_2}\right] (C(t_2)\Delta\hat{x}) + G(t_2)\Delta\hat{x} = AU(s). \tag{5}$$

We expand the t_2 dependence in a Fourier series, and using the Toeplitz matrix ($\mathbb{T}$) and vector ($\overset{\text{FD}}{\mathbb{V}}$) terminology from [13], we obtain a convenient matrix representation for the time-varying small-signal transfer function of the oscillator [14], [15]:

$$\underbrace{\left[\overset{\text{FD}}{\Omega}(s)\mathbb{T}_{C(t_2)} + \mathbb{T}_{G(t_2)}\right]}_{\overset{\text{HB}}{\mathbb{J}}(s)} \overset{\text{FD}}{\mathbb{V}}_{\Delta X}(s) = \overset{\text{FD}}{\mathbb{V}}_A U(s), \tag{6}$$

where $\overset{\text{FD}}{\Omega}(s) = \overset{\text{FD}}{\Omega} + sI$. $\overset{\text{HB}}{\mathbb{J}}(s)$ is often called the frequency-domain *conversion matrix* [14], [15].

Lemma 2.1: $\overset{\text{HB}}{\mathbb{J}}(s)$ loses rank by 1 $\forall s = ij\omega_0$, where ω_0 is the frequency of a free-running oscillator.

This implies that $\overset{\text{HB}}{\mathbb{J}}(s)$ is singular at DC and at every harmonics. Note that at DC (*i.e.*, s=0), $\overset{\text{HB}}{\mathbb{J}}(0)$ is actually the steady-state Jacobian of HB.

C. WaMPDE restores full rank to conversion matrix at DC

In the WaMPDE formulation, $\hat{x}$ captures the amplitude of circuit unknowns and $\omega(t_1)$ (the "local frequency") captures frequency changes explicitly and separately from the amplitude components. We assume that (3) has a unperturbed steady state solution $(x^*(t_2), \omega_0)$. Linearization of (3) around (x^*, ω_0) yields

$$\begin{aligned}\left[\frac{\partial}{\partial t_1} + \omega_0\frac{\partial}{\partial t_2}\right] (C(t_2)\Delta\hat{x}) + G(t_2)\Delta\hat{x} \\ +\Delta\omega(t_1)\frac{\partial}{\partial t_2} q(x^*) = Au(t_1).\end{aligned} \tag{7}$$

Following the same procedure as in Section II-B, we obtain a frequency-domain discretized system:

$$\begin{aligned}\underbrace{\left[\left(\overset{\text{FD}}{\Omega}(s)\mathbb{T}_{C(t_2)} + \mathbb{T}_{G(t_2)}\right),\ \ \overset{\text{FD}}{\mathbb{V}}_{\dot{q}^*(t_2)}\right]}_{\overset{\text{HB}}{\mathbb{J}}_A(s)} \begin{pmatrix}\overset{\text{FD}}{\mathbb{V}}_{\Delta X}(s) \\ \Delta\omega(s)\end{pmatrix} \\ = \overset{\text{FD}}{\mathbb{V}}_A U(s)\end{aligned} \tag{8}$$

$\overset{\text{HB}}{\mathbb{J}}_A(s)$ is the augmented Harmonic Balance Jacobian with offset s (or augmented conversion matrix). Compared with (6), $\overset{\text{HB}}{\mathbb{J}}_A(s)$ is augmented with the right column $\overset{\text{FD}}{\mathbb{V}}_{\dot{q}^*(t)}$.

Lemma 2.2: Augmenting $\overset{\text{HB}}{\mathbb{J}}(s)$ by a column $\overset{\text{FD}}{\mathbb{V}}_{\dot{q}^*(t)}$ ($\overset{\text{HB}}{\mathbb{J}}_A(s)$) restores full rank in the case $s = 0$ but not when $s = ji\omega_0$, for $i \neq 0$. Note that this augmented $\overset{\text{HB}}{\mathbb{J}}(s)$ at DC is actually the steady-state Jacobian of oscillator HB, augmented with a phase condition. Since it is not singular, standard oscillator HB succeeds.

III. Small signal linearization of the GeMPDE

For valid small-signal analysis, it is essential that the Jacobian matrix be full rank at *all* frequencies, not simply at $s = 0$. In this section, we propose a special Generalized MPDE (GeMPDE) formulation and prove that it solves the rank deficiency problem of the Jacobian matrix completely, via the use of new phase conditions. We first obtain a new small-signal transfer function under this formulation, and then show how both phase/frequency and amplitude characteristics of oscillators can be easily recovered from multi-time solutions.

A. The GeMPDE formulation

The GeMPDE, outlined in [10], is: :

$$\begin{aligned}\left[\hat{\Omega}(t_1,\cdots,t_d)\cdot\left[\tfrac{\partial}{\partial t_1},\cdots,\tfrac{\partial}{\partial t_d}\right]\right]q(\hat{x}(t_1,\cdots,t_d))\\ +f(\hat{x}(t_1,\cdots,t_d))=\hat{b}(t_1,\cdots,t_d)\end{aligned} \tag{9}$$

where d is the number of artificial time scales, the "phase" functions $\hat{\Phi}(t_1,\cdots,t_d)$ and the "local frequency" functions $\hat{\Omega}(\tau_1,\cdots,\tau_d)$ are defined as:

$$\hat{\Phi}(t_1,\cdots,t_d)=\begin{pmatrix}\tau_1\\ \vdots\\ \tau_d\end{pmatrix}=\begin{pmatrix}\hat{\phi}_1(t_1,\cdots,t_d)\\ \vdots\\ \hat{\phi}_1(t_1,\cdots,t_d)\end{pmatrix}, \tag{10}$$

$$\hat{\Omega}(\tau_1,\cdots,\tau_d)=\begin{pmatrix}\hat{\omega}_1(\tau_1,\cdots,\tau_d)\\ \vdots\\ \hat{\omega}_1(\tau_1,\cdots,\tau_d)\end{pmatrix}. \tag{11}$$

$\hat{\Phi}$ and $\hat{\Omega}$ is related by a nonlinear, implicit ODE

$$\left(\frac{\partial}{\partial t_1}+\cdots+\frac{\partial}{\partial t_d}\right)\hat{\Phi}(t_1,\cdots,t_d)=\hat{\Omega}\left(\hat{\Phi}(t_1,\cdots,t_d)\right). \tag{12}$$

This relation is the generalization of the fact that phase is the integral of local frequency.

Theorem 3.1: If $(\hat{\Omega},\hat{x})$ is a solution of (9), then the one-time waveform defined by $x(t)=\hat{x}(\hat{\Phi}(t,\cdots,t))$ solves the underlying DAE system, if $b(t)=\hat{b}(\hat{\Phi}(t,\cdots,t))$.

Proof: See [10]. ∎

B. Small signal linearization of the GeMPDE

To facilitate small-signal analysis, we use a special case of the GeMPDE. In this particular GeMPDE formulation, the frequency ω is treated as an extra explicit variable with two time scales, an internal warped scale (t_1) and an external unwarped time scale (t_2). The special bivariate GeMPDE form of (1) is:

$$\left[\frac{\partial}{\partial t_1}+\hat{\omega}(t_1,t_2)\frac{\partial}{\partial t_2}\right]q(\hat{x})+f(\hat{x})=b(t)=Au(t_1). \tag{13}$$

Lemma 3.1: If $(\hat{\omega},\hat{x})$ is a solution of (13), then the one-time waveform defined by $x(t)=\hat{x}(t,\hat{\phi}(t,t))$ solves the underlying DAE system if $b(t)=\hat{b}(t,\hat{\phi}(t,t))$, where $\hat{\phi}$ and $\hat{\omega}$ is related by:

$$\begin{aligned}\frac{\partial\hat{\phi}(t,t)}{\partial t}&=\frac{\partial\hat{\phi}(\tau_1=t,\tau_2=t)}{\partial\tau_1}+\frac{\partial\hat{\phi}(\tau_1=t,\tau_2=t)}{\partial\tau_2}\\ &=\hat{\omega}(t,\hat{\phi}(t,t)).\end{aligned} \tag{14}$$

Defining $\phi(t)=\hat{\phi}(t,t)$, we can rewrite the phase-frequency relation (14) as

$$\frac{d\phi(t)}{dt}=\hat{\omega}(t,\phi(t)). \tag{15}$$

This equation relates the multi-time frequency and the single-time phase variable. The single-time phase is then used to obtain a single-time solution from MPDE solutions using Lemma 3.1.

We now linearize this special case of the GeMPDE. We first note that the unperturbed steady state solution of the WaMPDE (3) $(x^*(t_2),\omega_0)$ also solves the GeMPDE (13). We can then linearize (13) around $(x^*(t_2),\omega_0)$ to obtain the linearized GeMPDE

$$\begin{aligned}\left[\frac{\partial}{\partial t_1}+(\omega_0+\Delta\omega(t_1,t_2))\frac{\partial}{\partial t_2}\right]q(x^*+\Delta\hat{x})\\ +f(x^*+\Delta\hat{x})=Au(t_1),\end{aligned} \tag{16}$$

i.e.,

$$\begin{aligned}\left[\frac{\partial}{\partial t_1}+\omega_0\frac{\partial}{\partial t_2}\right](C(t_2)\Delta\hat{x})+G(t_2)\Delta\hat{x}\\ +\Delta\omega(t_1,t_2)\frac{\partial}{\partial t_2}q(x^*)=Au(t_1).\end{aligned} \tag{17}$$

Following the same procedure as in Section II-B, we continue to obtain the frequency-domain discretized system

$$\begin{aligned}\underbrace{\left[\left(\overset{\text{FD}}{\Omega}(s)\mathbb{T}_{C(t_2)}+\mathbb{T}_{G(t_2)}\right),\quad\mathbb{T}_{\dot{q}^*(t_2)}\right]}_{\overset{\text{HB}}{\mathbb{J}}_{Ge}(s)}\begin{pmatrix}\overset{\text{FD}}{\mathbb{V}}_{\Delta X}(s)\\ \overset{\text{FD}}{\mathbb{V}}_{\Delta\omega}(s)\end{pmatrix}\\ =\overset{\text{FD}}{\mathbb{V}}_A U(s).\end{aligned} \tag{18}$$

Comparing with (8), we note that now the Jacobian is augmented by several more columns (N columns of $\mathbb{T}_{\dot{q}^*(t_2)}$, where N is the number of terms in truncated Fourier series). In this case, the size of $\overset{\text{HB}}{\mathbb{J}}_{Ge}(s)$ is $nN\times(n+1)N$, where n is the number of circuit unknowns.

Lemma 3.2: The augmented matrix $\overset{\text{HB}}{\mathbb{J}}_{Ge}(s)$ (augmenting $\overset{\text{HB}}{\mathbb{J}}(s)$ by columns of $\mathbb{T}_{\dot{q}^*(t_2)}$) is full rank at all frequencies.

This implies that $\overset{\text{HB}}{\mathbb{J}}_{Ge}(s)$ is non-singular at all frequencies. It further implies that if the perturbation signal is small, then both $\overset{\text{FD}}{\mathbb{V}}_{\Delta X}(s)$ $\overset{\text{FD}}{\mathbb{V}}_{\Delta\omega}(s)$ remain small. Therefore, linear small signal analysis of this special GeMPDE becomes valid.

C. New phase conditions

Since we have augmented $\overset{\text{HB}}{\mathbb{J}}(s)$ by N columns above, we have N more unknowns than equations. We then need N more equations in order to obtain a unique solution. We will term these equations *phase conditions*. While there is considerable apparent freedom in choosing phase conditions, they will need to satisfy a number of conditions in order to be useful from the standpoint of small-signal analysis. In particular, the phase condition rows that augment $\overset{\text{HB}}{\mathbb{J}}_{Ge}(s)$

1) must be of full rank themselves,
2) in addition to making the entire augmented Jacobian matrix full rank.

We now present the following phase condition equations which satisfy these characteristics:

$$\omega(t_1,t_2)\frac{\partial}{\partial t_2}\hat{x}_l=\frac{\partial x_{ls}(t_2)}{\partial t_2}, \tag{19}$$

where l is a fixed integer. $\hat{x}_l$ denotes the l^{th} element of $\hat{x}$, while x_{ls} is the l^{th} element of the steady state solution $x_s(t_2)$.

It is obvious that the unperturbed steady state $(x_l^*(t_2),\omega_0)$ satisfies (19). By linearizing around (x_l^*,ω_0) and expanding the t_2 dependence in Fourier series, we obtain:

$$\underbrace{\left[\overset{\text{FD}}{\Omega}\mathbb{T}_{e_l^T},\quad\mathbb{T}_{\dot{x}_l^*(t_2)}\right]}_{P}\begin{pmatrix}\overset{\text{FD}}{\mathbb{V}}_{\Delta X}(s)\\ \overset{\text{FD}}{\mathbb{V}}_{\Delta\omega}(s)\end{pmatrix}=0. \tag{20}$$

Lemma 3.3: The phase condition submatrix P is full rank at all frequencies.

This implies that the phase condition rows that augment $\overset{\text{HB}}{\mathbb{J}}_{Ge}(s)$ is full rank.

Putting the phase conditions and GeMPDE together, we obtain

$$\begin{bmatrix} \left(\overset{\text{FD}}{\Omega}(s)\mathbb{T}_{C(t_2)} + \mathbb{T}_{G(t_2)}\right), & \mathbb{T}_{\dot{q}^*(t_2)} \\ \overset{\text{FD}}{\Omega}\mathbb{T}_{e_l^T}, & \mathbb{T}_{\dot{x}_l^*(t_2)} \end{bmatrix} \begin{pmatrix} \overset{\text{FD}}{\mathbb{V}}_{\Delta X}(s) \\ \overset{\text{FD}}{\mathbb{V}}_{\Delta\omega}(s) \end{pmatrix} = \begin{pmatrix} \overset{\text{FD}}{\mathbb{V}}_A \\ z \end{pmatrix} U(s), \tag{21}$$

where $z = [0, ..., 0]^T$. The corresponding *small-signal transfer function* is:

$$\begin{aligned} \overset{\text{FD}}{\mathbb{V}}_H(s) &= \begin{pmatrix} \overset{\text{FD}}{\mathbb{V}}_{\Delta X}(s) \\ \overset{\text{FD}}{\mathbb{V}}_{\Delta\omega}(s) \end{pmatrix} / U(s) \\ &= \begin{bmatrix} \left(\overset{\text{FD}}{\Omega}(s)\mathbb{T}_{C(t_2)} + \mathbb{T}_{G(t_2)}\right), & \mathbb{T}_{\dot{q}^*(t_2)} \\ \overset{\text{FD}}{\Omega}\mathbb{T}_{e_l^T}, & \mathbb{T}_{\dot{x}_l^*(t_2)} \end{bmatrix}^{-1} \begin{pmatrix} \overset{\text{FD}}{\mathbb{V}}_A \\ z \end{pmatrix}. \end{aligned} \tag{22}$$

(22) is always nonsingular, for all frequencies.

D. Obtaining phase and amplitude characteristics

Once the transfer function is obtained (22), we can obtain $\overset{\text{FD}}{\mathbb{V}}_{\Delta X}(s), \overset{\text{FD}}{\mathbb{V}}_{\Delta\omega}(s)$ under perturbations of different frequencies. Multitime time-domain waveforms of Δx and $\Delta\omega$ at a given frequency can be obtained by performing inverse discrete Fourier transform. The phase characteristic can be recovered by the phase-frequency relation (15). To obtain the phase variation from $\Delta\omega$, we linearize (15) around (ϕ_0, ω_0). Using $\phi_0 = \omega_0 t$, we have

$$\frac{d\Delta\phi(t)}{dt} = \hat{\Delta\omega}(t, \omega_0 t + \Delta\phi(t)). \tag{23}$$

The one-time form of amplitude variation $\Delta x(t)$ can be recovered using *Lemma 3.1*:

$$\Delta x(t) = \hat{\Delta x}(t, \phi(t)), \tag{24}$$

where $\phi(t) = \omega_0 t + \Delta\phi(t)$. The overall solution of the oscillator is given by

$$x(t) = x^*(\phi(t)) + \hat{\Delta x}(t, \phi(t)), \tag{25}$$

where x^* is the steady state oscillatory solution.

In summary, the flow of the autonomous AC analysis process is outlined below:

flow of the autonomous AC analysis process

1) Solve for the steady state solution (x^*, w_0) using HB or shooting.
2) Calculate the transfer function numerically using (22).
3) Obtain multitime waveforms of Δx and $\Delta\omega$ at a given frequency.
4) Solve (23) numerically for phase variation.
5) Solve (24) numerically for amplitude variation.
6) Finally, generate the one-time solution using (25).

IV. Applications and Validation

In this section, we apply the GeMPDE-based small signal analysis to LC and ring oscillators. Comparisons with direct SPICE-like transient simulations confirm that our method captures oscillator phase/frequency and amplitude variations correctly. Speedups of orders of magnitude are obtained over SPICE-like transient simulation. We also verify OAC's capability of predicting injection locking in oscillators. All simulation were performed using MATLAB on an 2.4GHz, Athlon XP-based PC running Linux.

A. 1GHz negative-resistance LC oscillator

A simple 1GHz LC oscillator with a negative resistor is shown in Figure 1. At steady state, the amplitude of the inductor current is 1.2mA.

The circuit is perturbed by a current source in parallel with the inductor. Figure 2 shows frequency sweeps akin to standard AC analysis for both the capacitor voltage and the local frequency. Figure 3(a) shows the phase variation recovered from the bivariate form of frequency (using (23)) under a perturbation of $4\times10^{-5}sin(1.03w_0t)$. The one-time forms of amplitude variation of the capacitor voltage are shown in Figure 3(b). The capacitor voltage waveform is obtained using (25) and compared with full transient simulation in Figure 4. As can be seen, the results from our method match full simulation perfectly. A speedup of 15 times is obtained in this example.

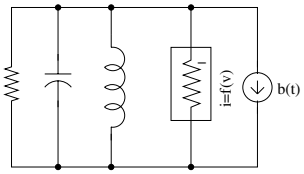

Fig. 1: A simple 1GHz LC oscillator with a negative resistor

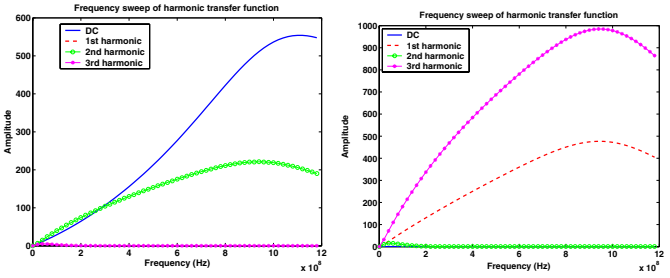

(a) Harmonic transfer functions of the capacitor voltage (b) Harmonic transfer functions of the local frequency

Fig. 2. Harmonic transfer functions: the frequency sweeps from DC to $1.2 \times 10^9 Hz$

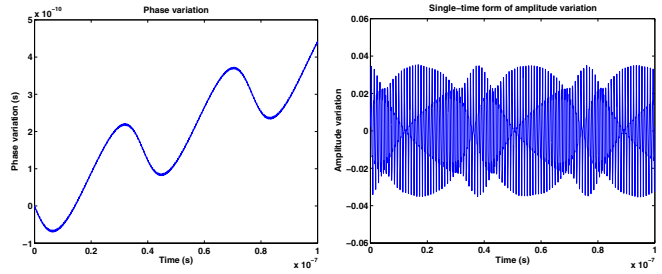

(a) Phase variation (b) One-time solution of amplitude variation

Fig. 3. Phase and amplitude variations of the capacitor voltage when the perturbation current is $4 \times 10^{-5}sin(1.03w_0t)$. The figure shows the simulation result for 100 cycles.

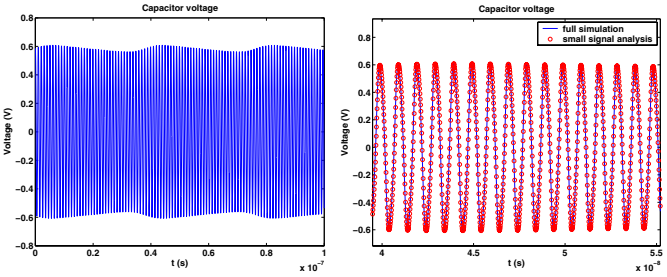

(a) Result recovered from small signal analysis (b) Detailed comparison (zoom in)

Fig. 4. Comparison of results from small signal analysis and full transient simulation (the perturbation current is $4 \times 10^{-5}sin(1.03w_0t)$).

We also test OAC for predicting injection locking. We use the perturbation frequency of $1.03\omega_0$; in this case, we expect the phase to change linearly with a slope of 0.03 (in our implementation , the

slope is scaled by $1/\omega_0$, so the slope is $\Delta\omega_0/\omega_0$). The perturbations are increased in strength to ensure that the oscillator is in lock. The phase variation from the small signal analysis is shown in Figure 5. Transient simulation results are also provided to verify that the oscillator is in lock. As can be seen in Figure 5, the phase variations from our method change as expected.

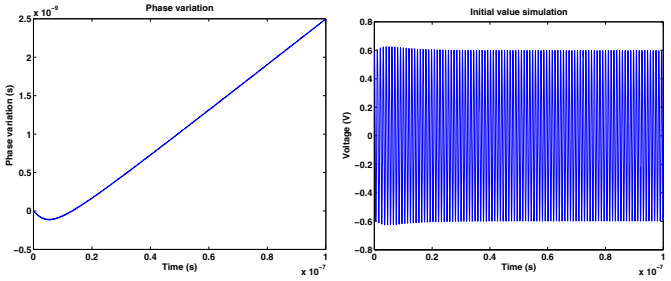

(a) Phase variation from small signal analysis

(b) Transient simulation result

Fig. 5. Oscillator in lock: the perturbation current is $8\times10^{-5}sin(1.03w_0t)$. The figure shows simulation result for 100 cycles.

B. 3 Stage ring oscillator

A 3 stage oscillator with identical stages is shown in Figure 6. The oscillator has a natural frequency of 1.53×10^5Hz. The amplitude of the steady-state load current is about 1.2mA.

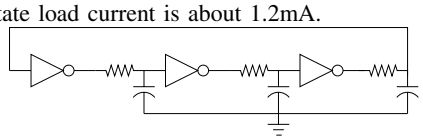

Fig. 6. A 3 stage oscillator with identical stages

Figure 7 shows AC analysis frequency sweeps for both the capacitor voltage and the local frequency of the oscillator under a perturbation current, connected in parallel with the load capacitor at node 1. Figure 8 shows the phase and amplitude variations at node 1. The waveform at node 1 is compared with full transient simulation in Figure 9. Again, we see perfect agreement between results from our method and transient simulation, with a speedup of 20× in this case.

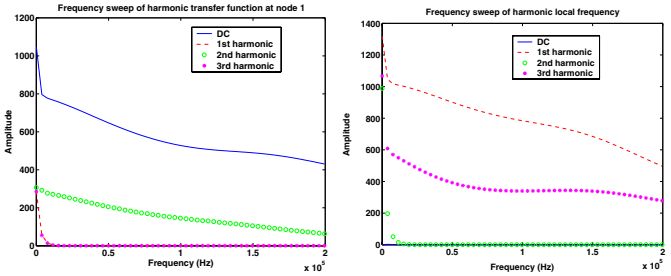

(a) Harmonic transfer functions at node 1

(b) Harmonic transfer functions of the local frequency

Fig. 7. Harmonic transfer functions: the frequency sweeps from DC to 2×10^5Hz

Figure 10 shows simulation results when the oscillator is in lock. We see that the phase changes linearly, as expected. Transient simulation results verify that the oscillator is indeed in lock.

C. 4GHz colpitts LC oscillator

A Colpitts LC oscillator is shown in Figure 11. The circuit has a free-running frequency of approximately 4GHz.

We perturb the oscillator with a small sinusoidal voltage source in series with L1. Figure 12 show frequency sweeps for both the current through L1 and the local frequency. Figures 13 shows the phase and amplitude variations of the current through L1. The waveform of the current through L1 is compared with full transient simulation

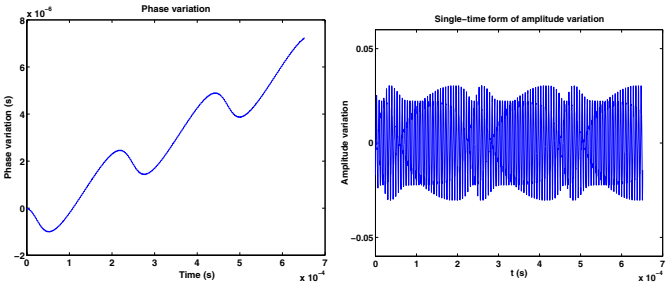

(a) Phase variation

(b) One-time solution of amplitude variation

Fig. 8. Phase and amplitude variations of the capacitor voltage when the perturbation current is $5\times10^{-5}sin(1.04w_0t)$. The figure shows simulation result for 100 cycles.

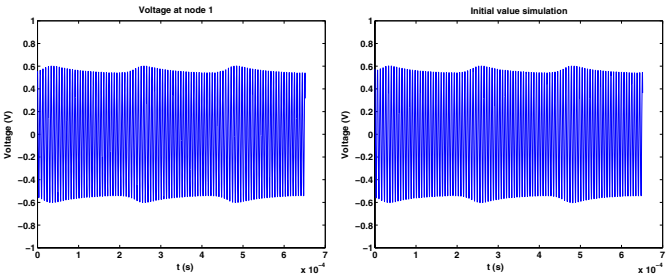

(a) Result recovered from small signal analysis

(b) Transient simulation result

Fig. 9. Comparison of the result from small signal analysis and full transient simulation (the perturbation current is $5\times10^{-5}sin(1.04w_0t)$).

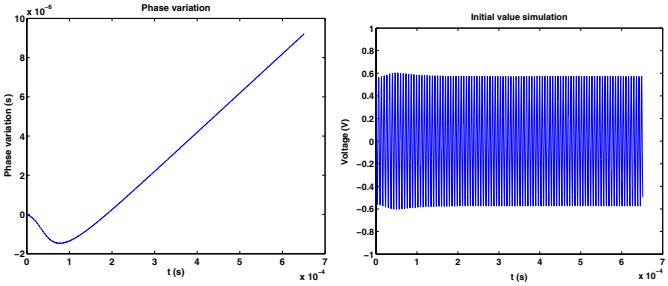

(a) Phase variation from small signal analysis

(b) Transient simulation result

Fig. 10. Oscillator in lock: the perturbation current is $5\times10^{-5}sin(1.02w_0t)$.The figure shows simulation result for 100 cycles.

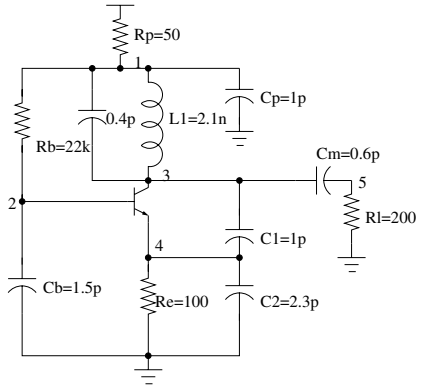

Fig. 11. A 4GHz Colpitts LC oscillator

in Figure 14. As can be seen, results from our method match full simulations perfectly. A speedup of 100 times is obtained in this example.

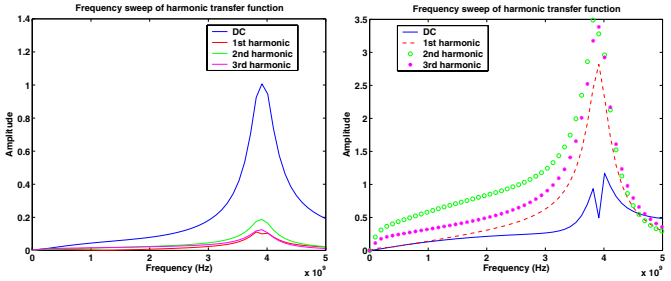

(a) Harmonic transfer functions of the current through L1

(b) Harmonic transfer functions of the local frequency

Fig. 12. Harmonic transfer functions: the frequency sweeps from DC to $5 \times 10^9 Hz$

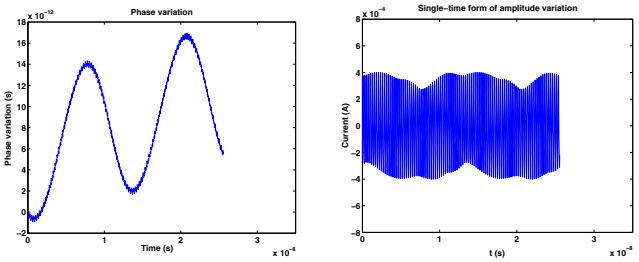

(a) Phase variation

(b) One-time solution of amplitude variation

Fig. 13. Phase and amplitude variations of the current through L1 when the perturbation current is $2 \times 10^{-3} sin(1.02 w_0 t)$. The figure shows simulation result for 100 cycles.

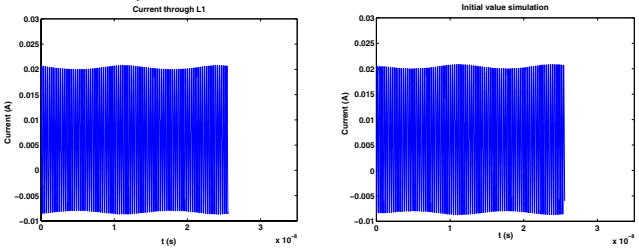

(a) Result recovered small signal analysis

(b) Transient simulation result

Fig. 14. Comparison of the result from small signal analysis and full transient simulation (the perturbation current is $2 \times 10^{-3} sin(1.02 w_0 t)$).

Figure 15 shows simulation results when the oscillator is in lock. Again, our method predicts injection locking correctly, as verified by transient simulation.

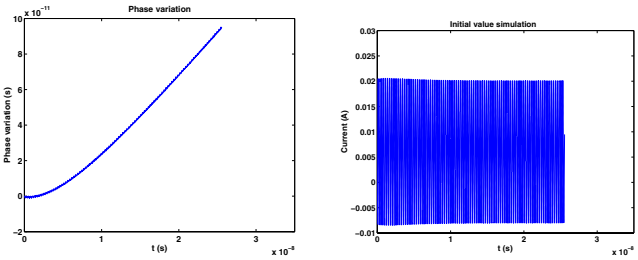

(a) Phase variation from small signal analysis

(b) Transient simulation result

Fig. 15. Oscillator in lock: the perturbation current is $4 \times 10^{-3} sin(1.005 w_0 t)$.The figure shows simulation result for 100 cycles.

V. Conclusions and Future Directions

We have presented a theory and computational algorithms for rigorously valid small-signal analysis of oscillators. Our technique is capable of capturing amplitude and frequency variations of oscillators under perturbations accurately, with large speedups over the full transient simulations that were the only prior alternative. Our OAC method is also able to predict injection locking in oscillators. We are currently extending our OAC to noise analysis, *i.e.*, analysis of oscillatory systems perturbed by random inputs. Stochastic analysis using the GeMPDE promises to be a powerful new tool that will significantly enhance theoretical and computational understanding of interesting and complex physical systems.

References

[1] L.W. Nagel. SPICE2: a computer program to simulate semiconductor circuits. PhD thesis, EECS department, University of California, Berkeley, Electronics Research Laboratory, 1975. Memorandum no. ERL-M520.

[2] Thomas L. Quarles. SPICE 3C.1 User's Guide. University of California, Berkeley, EECS Industrial Liaison Program, University of California, Berkeley California, 94720, April 1989.

[3] A. Demir, A. Mehrotra, and J. Roychowdhury. Phase noise in oscillators: a unifying theory and numerical methods for characterization. IEEE Trans. Ckts. Syst. – I: Fund. Th. Appl., 47:655–674, May 2000.

[4] R. Telichevesky, K. Kundert, and J. White. Receiver characterization using periodic small-signal analysis. In Proc. IEEE Custom Integrated Circuits Conference, May 1996.

[5] R. Telichevesky, K. Kundert, and J. White. Efficient AC and noise analysis of two-tone RF circuits. In Proc. IEEE DAC, pages 292–297, 1996.

[6] M. Okumura, T. Sugawara, and H. Tanimoto. An efficient small signal frequency analysis method of nonlinear circuits with two frequency excitations . IEEE Transactions on Computer-Aided Design of Integrated Circuits and Systems, 9:225–235, Mar 1990.

[7] M. Okumura, H. Tanimoto, T. Itakura, and T. Sugawara. Numerical Noise Analysis for Nonlinear Circuits with a Periodic Large Signal Excitation Including Cyclostationary Noise Sources. IEEE Trans. Ckts. Syst. – I: Fund. Th. Appl., 40(9):581–590, Sep 1993.

[8] J. Roychowdhury. Analyzing circuits with widely separated time scales using numerical PDE methods. IEEE Transactions on Circuits and Systems — I: Fundamental Theory and Applications, 48(5):578–594, 2001.

[9] H. G. Brachtendorf, G. Welsch, R. Laur, and A. Bunse-Gerstner. Numerical steady state analysis of electronic circuits driven by multi-tone signals. Electrical Engineering, 79:103–112, 1996.

[10] O. Narayan and J. Roychowdhury. Analysing Oscillators using Multitime PDEs. IEEE Transactions on Circuits and Systems — I: Fundamental Theory and Applications, 50(7):894–903, 2003.

[11] R. Adler. A study of locking phenomena in oscillators. Proc. Inst. Radio Eng., 34:351 – 357, Jun 1946.

[12] K. Kurokawa. Injection locking of microwave solid-state oscillators. Proc. IEEE, 61:1336 – 1410, Oct 1973.

[13] A. Demir and J. Roychowdhury. A Reliable and Efficient Procedure for Oscillator PPV Computation, with Phase Noise Macromodelling Applications. IEEE Transactions on Computer-Aided Design of Integrated Circuits and Systems, pages 188–197, February 2003.

[14] S.A. Maas. Nonlinear Microwave Circuits. Artech House, Norwood, MA, 1988.

[15] J. Roychowdhury, D. Long, and P. Feldmann. Cyclostationary noise analysis of large rf circuits with multitone excitations. IEEE J. Solid State Circuits, 33:324–336, Mar 1998.